J. Membrane Biol. 114, 159–173 (1990)

The Journal of
Membrane Biology

Electrical Tolerance (Breakdown) of the *Chara corallina* Plasmalemma: II. Inductive Property of Membrane and Effects of pH_o and Impermeable Monovalent Cations on Breakdown Phenomenon

Taka-aki Ohkawa and Izuo Tsutsui†
Department of Biology, College of General Education, Osaka University, Toyonaka, 560 Japan, and †Cell Physiology, National Institute for Physiological Sciences, Okazaki, 444 Japan

Summary. Changes in the chord conductance G and the membrane electromotive force E_m in the so-called breakdown region of large negative potential of the *Chara* plasmalemma were analyzed in more detail. In addition to the increase in G, the voltage sensitivity of the change in G increased, which was the cause of marked inductive current in the breakdown region. The breakdown potential, defined as a critical potential at which both low and high slope conductances of the I-V_m relationship cross, almost coincided with the potential at which an inductive current began to appear. This breakdown potential level changed with pH_o in a range between 5 and 9. The *Chara* plasmalemma was electrically most tolerant around pH_o 7.

In some cells E_m shifted to a positive level as large as +50 ~ +70 mV during the breakdown phenomenon. Such a large positive shift of E_m is caused mainly by the increase in conductance of Cl^- and partly Ca^{2+} and K^+.

Key Words *Chara* · DC conductance · electrical tolerance · electromotive force (E_m) · inductive property · kinetics of Cl^- channel

Introduction

A large inward current flows when the membrane potential V_m of the *Chara* plasmalemma is largely negative beyond a critical potential. Thus, the current-voltage (I-V_m) relationship shows a marked inward-going rectification in the V_m range more negative than the critical potential. This phenomenon in the *Chara* plasmalemma is generally called the breakdown phenomenon or sometimes called the punch-through (Coster, 1965) and the above critical potential is simply defined as the breakdown potential, BP (Ohkawa & Tsutsui, 1988*a*).

The large inward current during the breakdown phenomenon was supposed to be carried mainly by Cl^- (Coster & Hope, 1968). This increase in the Cl^- conductance, G_{Cl}, was suggested to be the cause of a large positive E_m shift (Ohkawa & Kishimoto, 1977). BP depends on external Ca^{2+} and also Ca^{2+}/Mg^{2+} ratio (Ohkawa & Tsutsui, 1988*a,b*). On the other hand, the activation of the Cl^- channel during excitation is mediated by the activation of the Ca^{2+}-binding protein calmodulin (Tsutsui, 1989).

The ionic process in living cell membranes has been classified sometimes in term of 'capacitative' and sometimes 'inductive'. The typical capacitative ionic process is the activation of the Na^+ channel in the squid giant axon membrane which causes a large Na^+ inward current, while the activation of the K^+ channel and the inactivation of the Na^+ channel are inductive which cause a large outward K^+ current and a decrease of Na^+ current (Hodgkin & Huxley, 1952; Cole, 1968). Mullins (1959) nicely discussed the mechanisms of the voltage dependence of the K^+ channel in the squid giant axon membrane and the inactivation of the Na^+ channel, by assuming that the membrane potential which yields a high electric field in the ion channels acts on the impermeable ions on the membrane capacitor. This exerts a mechanical force on the surfaces of both inner and outer membranes resulting in the mechano-electrical distortion of the structure of the ionic channels. A similar action of the electric field on the *Chara* plasmalemma might be effective, because the membrane impedance becomes markedly capacitative during excitation (Kishimoto et al., 1982). It can be inductive during the breakdown phenomenon (Coster & Smith, 1977; Beilby & Beilby, 1983). According to Ferrier, Dainty and Ross (1985), there are three possible mechanisms for the inductive property observed in the *Chara* plasmalemma: (*i*) voltage-dependent channel kinetics; (*ii*) electro-osmosis; and (*iii*) extracellular negative capacitance (i.e., inductance). However, we suppose that both the capacitative and inductive

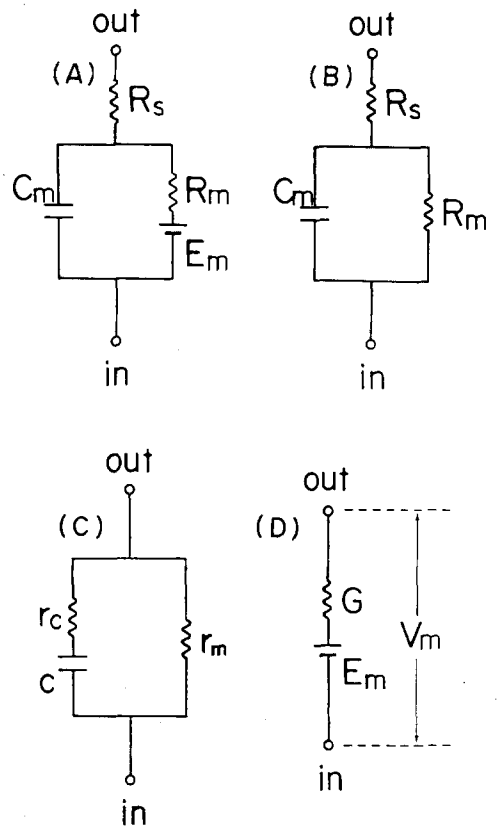

Fig. 1. Equivalent circuit of the membrane. (*A*) R_m: membrane resistance, i.e., reciprocal of membrane conductance G_m; E_m: membrane electromotive force; and R_s: resistance in series with the membrane. (*B*) Equivalent circuit in the case that the change in G_m during impedance measurement is very small. (*C*) Equivalent circuit which is electrically equal to circuit B. As for r_s, c_m and r_m, *see* the text. (*D*) A simplified Thèvenin model. *G*: instantaneous DC conductance; and V_m: membrane potential

properties of the *Chara* plasmalemma should originate from the voltage- and time-dependent kinetics of the Cl^- channel controlled by Ca^{2+}.

The present experiments were carried out intending, first to determine the DC conductance of the membrane having an inductive property, and second to determine the effects of pH_o and external monovalent cations such as K^+ and Na^+ on the breakdown phenomenon. The experiments on the effect of pH_o were carried out expecting competition between H^+ and Ca^{2+} at the same Ca^{2+} binding site, i.e., expecting to get a result similar to the increase in Mg^{2+} at a constant Ca^{2+} concentration (Ohkawa & Tsutsui, 1988*a*,*b*). In other words, a decrease in pH_o would cause a decrease in the electrical tolerance. Efforts were also made to determine to what extent Na^+ and K^+ participate in the large inward current as ion carriers during the breakdown phenomenon.

Equivalent Circuits

Figure 1*A* shows a simplified equivalent circuit of the *Chara* membrane. Since there are various voltage-dependent ion channels such as the K^+ channel (Kitasato, 1973; Beilby, 1986; Fisahn, Hansen & Gradmann, 1986*a*; Ohkawa, Tsutsui & Kishimoto, 1986; Sokolik & Yurin, 1986) and electrogenic H^+ pump (Beilby, 1984; Kishimoto et al., 1984; Takeuchi et al., 1985; Fisahn, Mikschl & Hansen, 1986*b*; Kami-ike et al., 1986), the membrane conductance G_m (= $1/R_m$) should also be voltage dependent. Each voltage-dependent channel would reach respective new steady state according to receptive relaxation times, depending on both the amplitude and the sign of the step change in V_m. Accordingly, the change in G_m is generally time- as well as voltage-dependent. Since E_m is a function of G_m (*see* Appendix), the change in E_m is also time and voltage dependent.

On the other hand, if a voltage or a current perturbation for the membrane impedance measurement is moderate and its effects on the voltage-dependent conductances are so small that we can neglect the change in the membrane impedance, then we can also neglect the change in E_m caused by the electrical perturbation. In such a case, i.e., during restricted duration of the impedance measurement, equivalent circuit A can be approximated by circuit B. Equivalent circuit C is electrically entirely equal to circuit B. The relations between the parameters of both circuits B and C are as follows;

$$r_m = R_s + R_m \tag{1}$$

$$r_c = R_s \cdot (R_s + R_m)/R_m \tag{2}$$

$$c_m = C_m \cdot [R_m/(R_s + R_m)]^2. \tag{3}$$

When we use a moderate amplitude of square shape voltage pulse (v_o) to determine the membrane impedance under voltage clamp conditions, the current on-response (i_{on}) should be as follows;

$$i_{on} = v_o \cdot [1/r_m + (1/r_c) \cdot \exp(-t/\tau_c)] \tag{4}$$

where

$$\tau_c = r_m \cdot c_m \tag{5}$$

$$= R_m \cdot C_m \cdot [R_s/(R_s + R_m)]. \tag{6}$$

At the steady state the amount of on-response (i_s) is as follows:

$$i_s = v_o/r_m. \tag{7}$$

DC conductance G [= $1/r_m = 1/(R_s + R_m)$] is determined as:

$$G = i_s/v_o = 1/r_m. \tag{8}$$

Note that the pulse duration necessary for observing i_s depends on the time constant τ_c. When v_o is turned off at $t = t_0$ after i has become i_s, the off-response (i_{off}) in this case is as follows:

$$i_{off} = -(v_o/r_c) \cdot \exp[-(t - t_0)/\tau_c]. \tag{9}$$

If we can use v_o of a short duration due to a small τ_c[1], G can be measured almost instantaneously. Consequently, the thus determined DC conductance G may be called an instantaneous chord conductance. In other words, the instantaneous chord conductance G is a DC conductance which should be determined in a restricted short duration by using a moderate amplitude of voltage pulse at any given V_m level. Under such restricted conditions at a given V_m level, equivalent circuit A can be replaced with the simple Thèvenin model D and the relationship between I and V_m in equivalent circuit D is as follows:

$$I = G \cdot (V_m - E_m). \tag{10}$$

E_m can be calculated as

$$E_m = V_m - I/G. \tag{11}$$

Material and Methods

Internodal cells of *Chara corallina*, 2 ~ 6 cm in length and 500 ~ 1000 μm in diameter, were used throughout the experiments. The internodal cells were kept in APW[2] for over 15 hr before the experiments. The ionic composition of standard APW (*s*-APW) was (in mM): 0.5 KCl, 0.2 NaCl, 0.1 $CaCl_2$, and 0.1 $MgCl_2$. The pH of *s*-APW (pH_o) was adjusted to 7 with 5 mM TES and NaOH. APWs of pH_o = 5 and 9, having the same ionic compositions and concentrations as *s*-APW, were also prepared by using 5 mM MES and 5 mM Tricine, respectively. APWs of different pH_o between 5 and 9 were prepared by mixing *s*-APW with either the APW of pH_o = 5 or 9. Other solutions will be described wherever needed.

The potential and current measuring methods, voltage-clamp methods[3], and other measuring systems were almost the same as described previously (Kishimoto et al., 1982; Ohkawa & Tsutsui, 1988*a*). Briefly, the membrane potential V_m was changed from the resting potential to a more negative potential either stepwisely or linearly and slowly (−100 mV/60 sec: this rate yields almost a steady-state I-V_m relationship; Ohkawa & Tsutsui, 1988*a*) with a programmable waveform generator (NF Electronic Instrument, Intelligent/Arbitrary Synthesizer 1731). A series of 32 voltage pulses (test pulses) of square shape and of a few tens of msec in duration was superimposed on a stepwise or a slow ramp potential change to know G and E_m. The initial two test pulses were used to determine G values at rest and the third test pulse was used to start either the stepwise potential or the ramp potential change.

The current response i, test pulse v_o, and trigger pulse were A/D converted with a data acquisition system (MDAS 8A, Datel) having eight input channels and were recorded with a digital cassette tape recorder (MT-2, TEAC) and also with a floppy disk drive (YE DATA). In the present experiments, 128 data points in each current response against each test pulse were sampled at about 1-msec interval. v_o, i and their ratio were computed by using a program (BASIC) developed by Dr. N. Kami-ike. They were also plotted on a plotter (Iwatsu Electric, SR-6602). The G was usually determined as the ratio of the value of steady-state current (i_s) of each on-response to the amplitude of test voltage pulse (v_o). However, if the inductive current response was apparently recorded, the ratio of the minimum value (i_m) of the on-response to v_o was used for the determination of G (*see* Determination of G and Estimation of E_m in Results).

Results

Current Pattern and Current Responses During a Large Negative Shift of V_m

Figure 2*A* (right panel) shows the current pattern I, which was obtained when V_m shifted slowly and linearly from the resting level (−219 mV) to a large negative level (−405 mV) (left panel). The I-V_m relationship replotted from Fig. 2*A* is shown in Fig. 4 (uppermost). When V_m moves to the negative side beyond a critical level (−387 mV), a marked inward current flows. This critical potential is simply defined as breakdown potential (BP; Ohkawa & Tsutsui, 1988*a*). When voltage clamp conditions are suddenly released from V_m = −405 mV (under this condition I is zero), V_m jumps almost instantaneously from the large negative potential (−405 mV) to a large positive level, the peak of which is +71 mV[4], and comparatively rapidly returns to a slightly negative level (−20 mV) (left panel of Fig. 2*A*. The latter V_m level almost coincided with the peak of action potential of this cell. Then, the membrane repolarizes slowly to the resting level, which usually took about 10–30 min.

Actually, to determine both G and E_m during such a large negative shift of V_m, a square test pulse (v_o) of −13.5-mV amplitude and 38.5-msec duration was repeatedly superimposed on the slow V_m shift. Current responses (i) to v_o at eight different V_m levels are exhibited in Fig. 2*B*. In the whole V_m range i

[1] Since the range of τ_c is between 0.6 and 5 msec, the range of t_0 is roughly between 10 and 50 msec.

[2] *Abbreviations:* APW, artificial pond water; BP, breakdown potential; MES, 2-(N-morpholino)ethanesulfonic acid; TES, N-Tris(hydroxymethyl)methyl-2-aminoethanesulfonic acid; TMA-Cl, tetramethylammonium chloride; TMA-OH, tetramethylammonium hydroxide; and Tricine, Tris(hydroxymethyl) methylglycine.

[3] In the present series of voltage clamp experiments we did not compensate R_s value. R_s value which was determined by using a step current under current clamp conditions was actually in the range between 0.5 and 1.2 kΩ · cm². Thus, a current of I causes a voltage shift by $I \cdot R_s$. However, the effect of such uncompensated R_s on the accuracy of a clamped potential is not important for a qualitative analysis of the present paper.

[4] This peak seemed to be more positive than +71 mV in some cells, but, in most cases less negative than the peak of action potential.

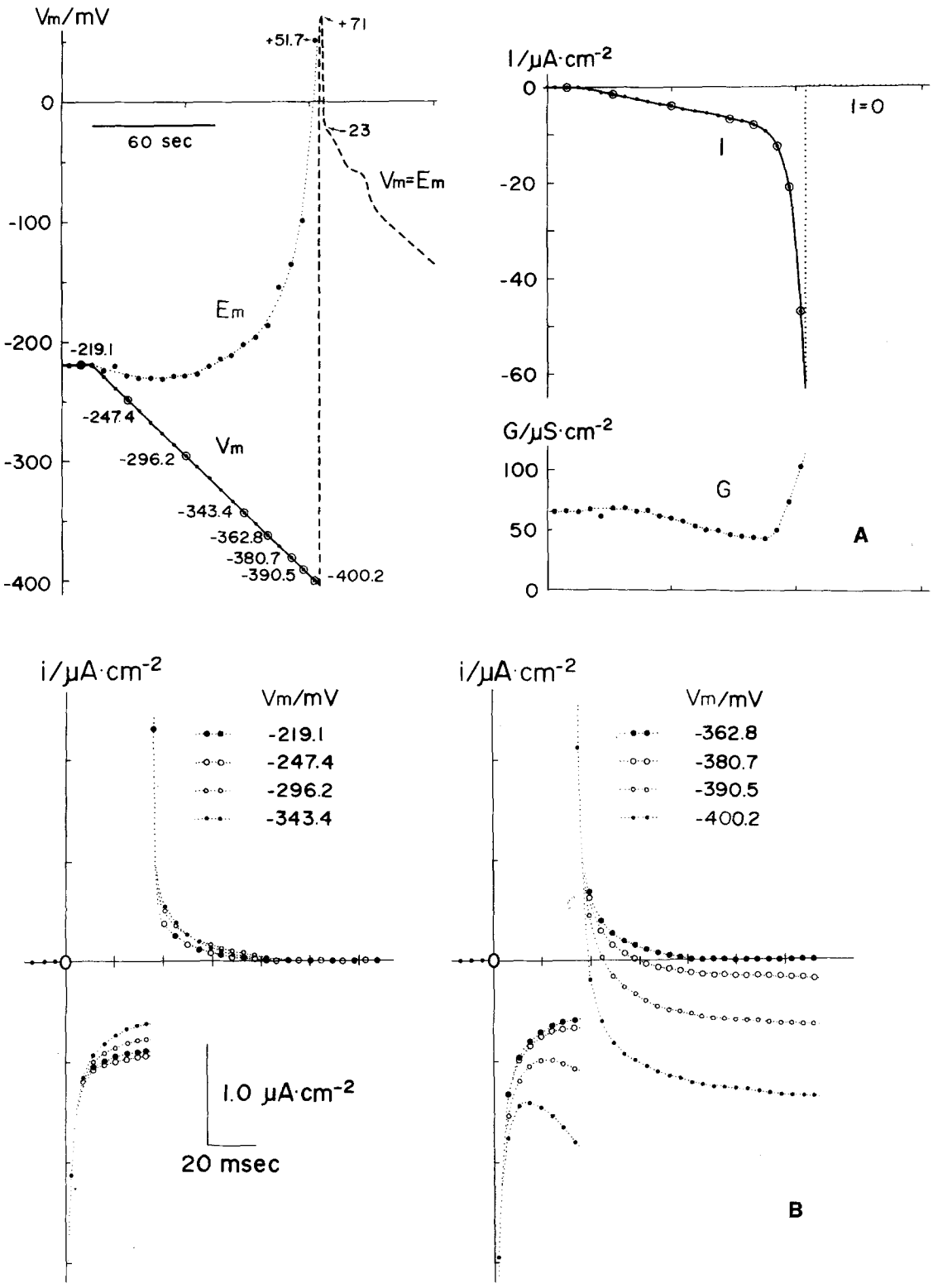

Fig. 2. (*A*) Left panel: A slow negative V_m shift under voltage clamp conditions and change in E_m. Right panel: Current pattern I and DC conductance G. G and E_m were determined as described in text. (*B*) Current responses i to v_o at different V_m levels. At respective dotted (●) V_m levels shown in *A* a square shape test voltage pulse v_o (−13.5 mV in amplitude and 38.5 msec in duration) was superimposed. Left panel: Current responses at four different V_m levels ((⊙) in *A*) in the region less negative than the breakdown potential (BP). Right panel: Current responses at four different V_m levels ((⊙) in *A*) in the region around and more negative than BP

shows a large negative on-spike[5] and a large positive off-spike.[5] In the V_m range less negative than −365 mV the on-spike decays to a steady state, while the off-spike to zero. Such on- and off-responses of i can be qualitatively expected from Eqs. (4) and (9). Nevertheless, in the V_m range more negative than −385 mV (i.e., about BP) the on-response shows an increase in the inward current either from a steady state or during the decay to a steady state. Concomitantly, the off-response shows a negative tail current. Such a current response to a square voltage pulse can be called inductive in the sense that the current response lags behind the test voltage signal, while the decay of i can be capacitive in the reverse sense.

Determination of G and Estimation of E_m

In Fig. 2*B* the inductive current is more marked when V_m is more negative than BP. To determine the G value of the membrane having such a marked inductive property, the possibility of the existence of a simple ohmic linear relationship between v_o and i was explored by examining on-responses to different v_o at the steady state of $V_m = -375$ mV (Fig. 3, inset). The current responses are shown in Fig. 3*A* (left and right panels).

In Fig. 3*A*, when v_o is smaller than −18.2 mV, the inductive current response is not appreciable. However, v_o of −25.6 mV causes a slight inductive current, while a larger v_o causes a marked one. Thus, we can easily suppose that both the steady-state current and the time constant of the inductive process are voltage dependent.

The time constant of the capacitive current ($\tau_c = 0.6 \sim 5.0$ msec) is usually much smaller than that of the inductive current ($\tau_1 >$ a few tens of msec: *see* Discussion). Therefore, it is possible to select a suitable period of time during which both capacitive and inductive currents are small. In such a moderate time i should be usually minimal. Thus, the minimum amount of on-responses (i_m) is plotted against different v_o (Fig. 3*B*). Since the i_m-v_o relationship yields a straight line in Fig. 3*B*, the following equation for this line was obtained by using the least square method (broken line in Fig. 3*B*):

$$i_m = 28.20 \cdot (v_o - 1.90)/1000, \tag{12}$$

where 28.20 is in $\mu S/cm^2$, v_o in mV, and i_m in $\mu A/cm^2$. 1.90 mV in Eq. (12) corresponds to a small positive E_m shift.

Similarly, another straight line which might cross the 0-0 point could also be supposed. The equation for this straight line (solid line in Fig. 3*B*) is as follows:

$$i_m = 30.00 \cdot v_o/1000. \tag{13}$$

Equation (13) implies the assumption that during the impedance measurement the change in G is so small that the change in E_m could be neglected. On the other hand, Eq. (12) implies that the change in G during the impedance measurement affects the estimation of E_m. The value of G in this paper is fundamentally based on the former assumption (i.e., Eq. (13)). That is, we adopted the ratio of i_m to v_o as the value of G without showing detailed time analysis of current response.

G (Fig. 2*A*, right panel) is replotted against V_m in Fig. 4 (bottom). In Fig. 4, G decreases slightly between the resting level and a fairly negative level (about −370 mV), but it increases in the V_m region more negative than −380 mV, where the inward current is marked (i.e., breakdown region). However, note that G in the breakdown region is not as large as expected from the slope conductance of the I-V_m relationship (uppermost).

E_m calculated from Eq. (11) is plotted in Fig. 2*A* (left), which is replotted against V_m in Fig. 4 (middle). E_m shifts slightly toward negative in the V_m region less negative than −300 mV, while it shifts markedly toward positive direction in the V_m region more negative than about −380 ~ −390 mV. The V_m level at which E_m began to shift toward positive direction was usually less negative than that at which the increase in G started. In Fig. 2*A* it is worth mentioning that the calculated E_m (+51.7 mV) just before the release of voltage clamp conditions at $V_m = -400.2$ mV continues up to V_m (= E_m = +71.0 mV) just after the release. The slight discrepancy between the calculated E_m just before and V_m just after the release from voltage clamp conditions is mainly due to the neglect of change in G during the impedance measurement[6].

[5] R_s of this series of experiments determined by using a step current under current clamp conditions was 1.11 kΩ · cm². According to Eqs. (4) or (9), theoretically this amount of R_s should cause the on- and off-spikes of 12.27 $\mu A/cm^2$ (since $|v_o|$ is 13.5 mV, $|v_o|/R_s$ is 12.27 $\mu A/cm^2$). Thus, both on- and off-spikes are usually too large. Besides, their responses are too fast. Accordingly, both spikes cannot be recorded simultaneously together with much slower process and also they cannot be analyzed with the same accuracy as the steady state value of i_{on}.

[6] In the case of Fig. 3, I is about −10 $\mu A/cm^2$ at $V_m = -375$ mV. The E_m estimated by using a G value of 28.20 $\mu S/cm^2$ (Eq. (12)) is −20.4 mV. However, the E_m is −41.7 mV if we adopt 30.00 $\mu S/cm^2$ as a G value (Eq. (13)).

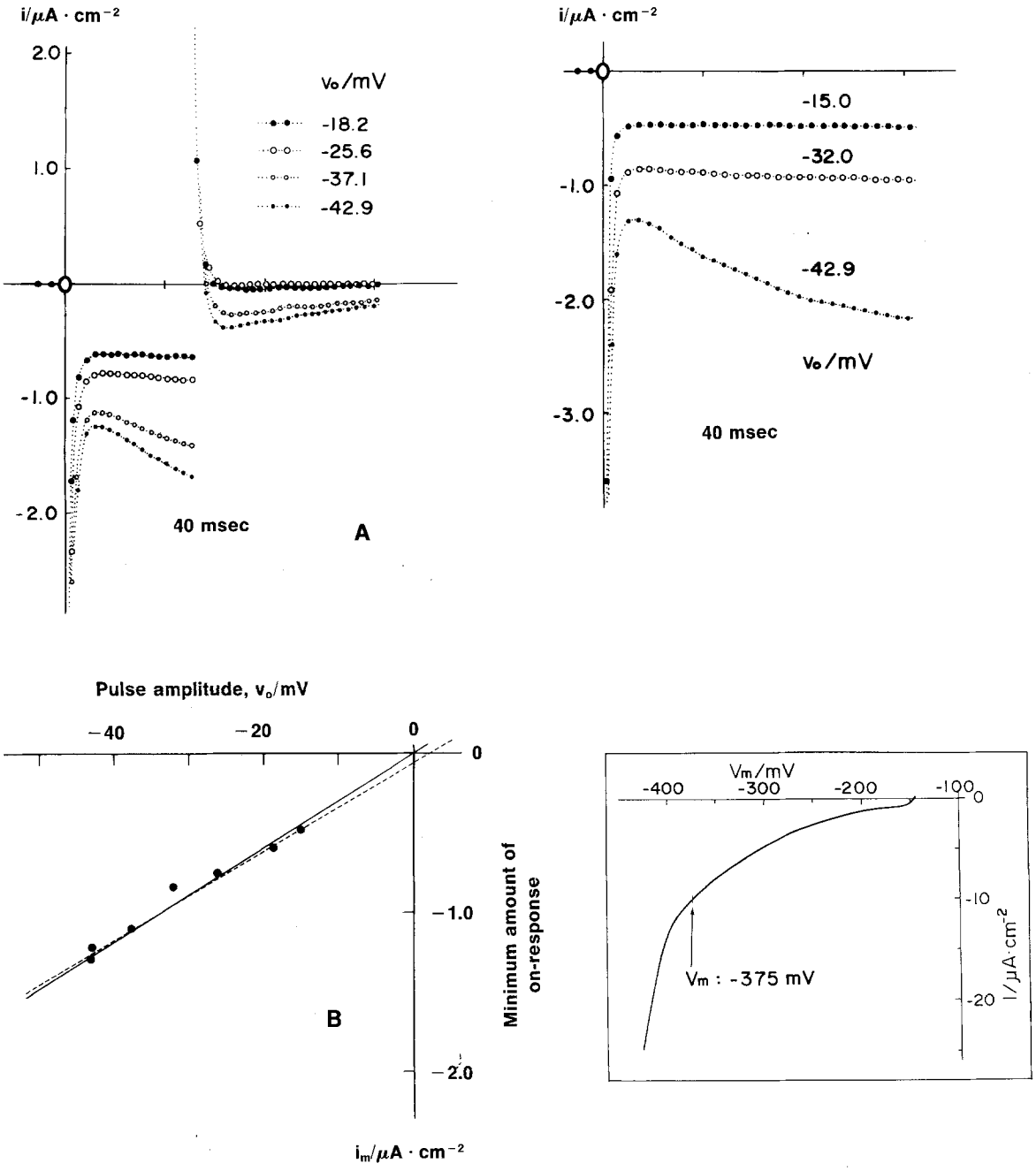

Fig. 3. Current responses i to v_o of different amplitudes and durations. Inset: The I-V_m relationship under a slow ramp potential control. Almost at the steady state at $V_m = -375$ mV (vertical line at $V_m = -375$ mV), a series of v_o of different amplitudes was superimposed. (*A*) Left panel: Pulse duration is 38.5 msec. Right panel: Pulse duration is 140 msec. (*B*) i_m-v_o relationship. i_m: The minimum value of i_{on} shown in *A*. Solid line: $i_m = 30.00 \cdot v_o/1000$ μA/cm². Broken line: $i_m = 28.20 \cdot (v_o - 1.90)/1000$ μA/cm². 30.00 and 28.20 are in μS/cm² and v_o in mV. The sample was different from that shown in Fig. 2

Does the Inductive Current Flow with a Dead Time?

If the inductive current begins to flow with a voltage-dependent dead time (i.e., delay), the inductive current in Fig. 3*A* might start to flow much later, even if v_o is small. However, the prolongation of v_o in such a time range as shown in Fig. 3*A* did not always cause an apparent inductive current. Thus, whether some properties of the dead time of the inductive current can be found or not was tested by examining how the negative tail current of the off-

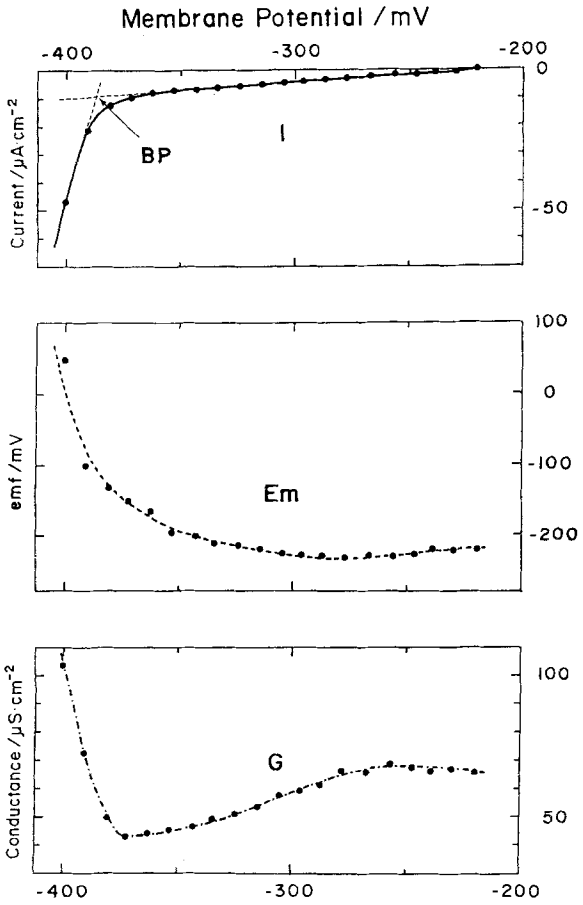

Fig. 4. Voltage dependences of I, E_m, and G. These curves are replotted from Fig. 2*A*. Uppermost: I-V_m relationship. BP is the breakdown potential. Middle: E_m (emf)-V_m relationship. Bottom: G-V_m relationship

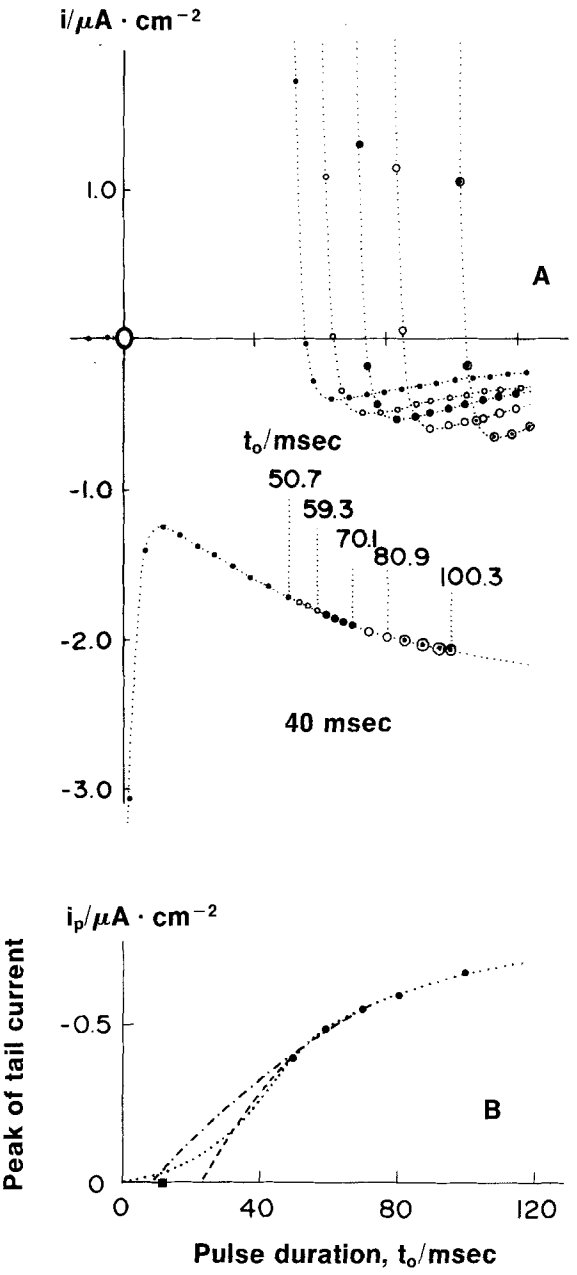

Fig. 5. Off-current responses. The experiment was carried out at the same V_m level (i.e., −375 mV) in the same sample as shown in Fig. 3. (*A*) Current response i. i to six different durations t_0 of v_o are superimposed. The amplitude of every v_o was kept constant at −42.9 mV. (*B*) i_p–t_o relationship. i_p: peak of the tail current of the off-response. (●): Data points from the five peaks. (■): The time at which i_{on} is minimum. Three curves were drawn by eye

response depends on the duration (t_0) of v_o. For this purpose, an amplitude of v_o was chosen which was large enough so that the inductive property could be easily observed[7]. The result of one of such off-response experiments is shown in Fig. 5*A*, the data of which were obtained at the same V_m level (i.e., −375 mV) of the cell shown in Fig. 3, inset. Here, v_o was fixed to −42.9 mV and six different durations of t_0 were applied (50.7, 59.3, 70.1, 80.9, 100.3 and 140 msec). The interval between two test pulses was about 700 msec. Five different off-responses having different durations are superimposed in Fig. 5*A*. The peak of the negative tail current (i_p) is plotted against the duration t_0 (Fig. 5*B*). When t_0 decreases, i_p decreases apparently exponentially. As shown in the figure, the i_p-t_0 curve can be extrapolated to t_0 of either between 9 (-·-·-) and 22 msec (----) or to 0 msec (·····) showing a sigmoid shape. The latter suggests that the inductive current may begin to flow without a dead time, while the former suggests that a dead time of 9 ~ 22 msec may be necessary for the initiation of the inductive current. In the

[7] The amplitude of v_o chosen for this experiment was much larger than that usually used for impedance measurement.

Table 1. Breakdown potentials (BPs) and BP/BP^{p7} ratios at different pH_o[a]

	BP (mV)							
Cell no.	pH_o							Ca^{2+}/Mg^{2+} (mM ratio)
	5.0	6.0	6.5	7.0	7.5	8.0	9.0	
				−443.0[1]				
87BRpH01	−372.5[2]			−438.0[3]		−416.4[4]		0.1/0.1
				−460.4[5]				
				av: −447.2				
87BRpH02	−346.9[3]			−415.0[1]			−363.1[2]	0.1/0.1
				−428.0[1]				
87BRpH03	−367.3[3]	−443.2[2]		−423.8[4]			−360.4[5]	0.1/0.1
				av: −425.9				
				−395.2[1]				
87BRpH04				−391.2[4]		−375.9[2]	−356.9[3]	0.1/0.1
				av: −393.2				
				−431.1[1]				
87BRpH05	−363.8[2]	−415.5[4]		−426.8[3]				0.1/0.1
				−432.1[5]				
				av: −430.0				
87BRpH06	−396.6[4]			−463.8[1]		−429.3[3]	−346.0[2]	0.1/0.1
87BRpH07	−393.2[3]	−434.5[2]		−435.4[1]				0.1/0.1
				−448.3[1]		−399.0[2]		
87BRpH08				−443.2[3]		−441.4[4]	−400.0[5]	0.1/0.1
				av: −445.8		av: −420.2		
				−450.0[1]				
87BRpH09	−344.0[2]			−449.2[3]		−398.3[4]	−322.4[5]	0.1/0.1
				−419.0[6]				
				av: −439.4				
				−412.0[1]				
87BRpH10			−385.0[4]	−408.0[3]		−390.0[2]		0.1/0.1
				av: −410.0				
87BRpH11				−368.0	−370.0			0.1/0.1
87BRpH11				−348.0	−318.5			0.03/0.1
87BRpH11				−395.0	−387.0			0.3/0.1
87BRpH11				−413.5	−379.0			1.0/0.1
87BRpH12				−3.82.5	−381.7			0.1/0.1
87BRpH12				−351.7	−373.0			0.03/0.1
87BRpH12				−430.8	−433.3			0.3/0.1
87BRpH12				−445.8	−443.3			1.0/0.1
			−350.0[2]	−375.0[1]				
87BRpH13			−333.3[4]	−415.5[3]				0.1/0.1
			−370.0[6]	−397.2[5]				
			av: −351.1	av: −395.9				
			−351.7[2]	−378.2[1]				
87BRpH13			−316.7[4]	−378.8[3]				0.03/0.1
			−377.8[6]	−383.0[5]				
			av: −348.2	av: −380.0				
87BRpH13			−427.5	−428.3				0.3/0.1

[a] The number of each superscript means the order of the experiment in each series. Ca^{2+}/Mg^{2+} ratio is varied for three samples (87BRpH11-13). av: average.

latter case, the capacity current of the off-response might actually mask the inductive current when t_0 is small.

The above simple experiment could not make it clear whether the inductive current begins to flow with a dead time or not. At present, however, we suppose that it is not necessary to take a dead time for the initiation of inductive current into account, because the simulation for the inductive current is well fitted without a dead time (*see* Fig. 10).

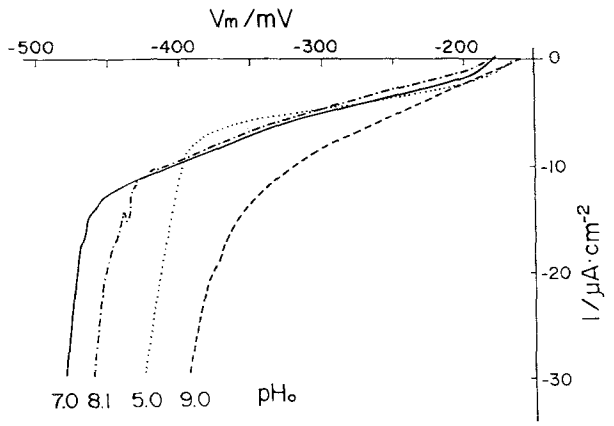

Fig. 6. I-V_m relationships at different pH_o. These curves are from cell number 87BRpH06 in Table 1

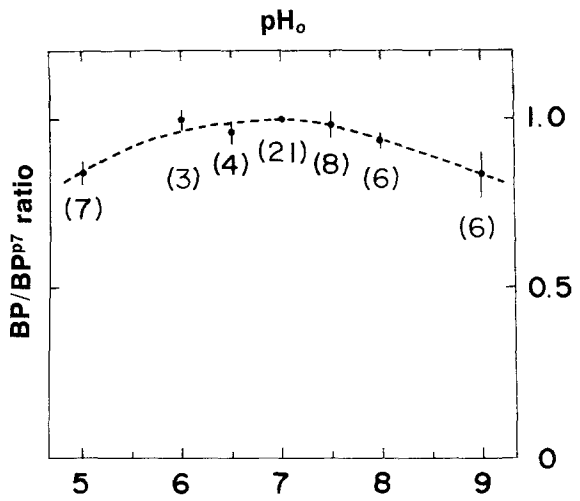

Fig. 7. BP/BP^{p7}-pH_o curve. BP: breakdown potential. BP^{p7}:BP at pH_o = 7. The average of the BP/BP^{p7} ratio in Table 2 was plotted against pH_o. The solid line was drawn by eye

pH_o Dependence of BP

As described in Fig. 2*B*, BP almost coincided with the V_m level at which the inductive current began to appear. On the other hand, the level of BP mainly depends on both Ca^{2+}, which is necessary for the maintenance of membrane electrical tolerance (Ohkawa & Tsutsui, 1988*a*,*b*), and the ratio of Ca^{2+} to Mg^{2+}. From the viewpoint of competition between H^+ and Ca^{2+} at the Ca^{2+} binding site, we expected that the increase in pH_o would cause an increase in the electrical tolerance. Several I-V_m relationship curves which were obtained by varying pH_o in the range between 5 and 9 are shown in Fig. 6. The pattern of each I-V_m relationship is essentially the same, but the breakdown region shifts depending on pH_o, and at pH_o = 7 the breakdown region is situated on the most negative side.

BPs at different pH_o are listed in Table 1, which were compared to BP at pH_o = 7 (BP^{p7}). The BP/BP^{p7} ratios are listed in Table 2 and also plotted against pH_o in Fig. 7. The BP/BP^{p7} ratio has a peak around pH_o = 7.

Effects of Exchange of Na^+ and K^+ for Impermeable Ions on the Breakdown Phenomenon

To know whether Na^+ affects the breakdown phenomenon or not, Na^+-free APW was prepared by exchanging NaCl for either choline chloride or tetramethylammonium chloride (TMA-Cl) and NaOH for choline- or TMA-hydroxide. The exchange of Na^+ for these cations had very little effect on both resting potential and I-V_m relationship (Fig. 8).

On the other hand, replacing K^+ in APW with

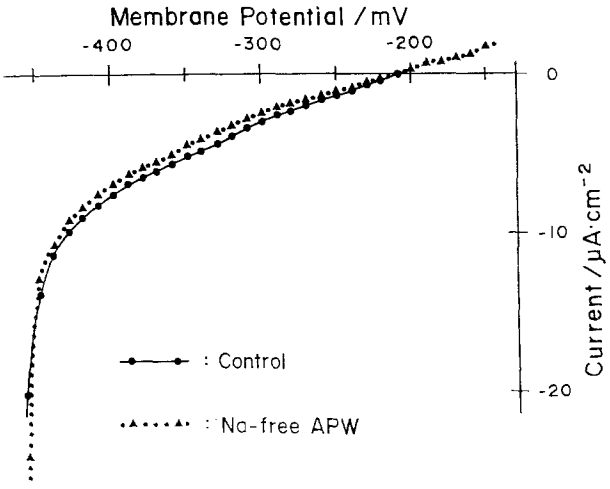

Fig. 8. Effect of Na^+ on the breakdown phenomenon. This experiment was carried out by exchanging NaCl for choline chloride and NaOH for TMA-OH. The I-V_m relationship in Na-free APW is compared to the control one

Cs^+, a typical K^+ channel blocker, made the resting potential more negative by about 20 ~ 50 mV and decreased the inward current in the whole V_m range without a marked change in BP level (Fig. 9). The I-V_m relationship in the K-free (Cs) APW (-▲--▲--) shows a more marked inward-going rectification. Since the decrease of this inward current is mainly due to a decrease of the inward K^+ current (I_K), the differential I-V_m relationship, which is obtained by subtracting the I-V_m relationship in K^+-free (Cs) APW from the control one (in the standard APW), corresponds to the I_K-V_m relationship. In Fig. 9 such an I_K-V_m relationship (··■····■··) is shown together with both the I-V_m relationship in K^+-free

Table 2. BP/BP^{p7} ratios at different pH_o[a]

Cell no.	BP/BP^{p7}							Ca^{2+}/Mg^{2+} (mM ratio)
	pH_o							
	5.1	6.1	6.5	7.0	7.5	8.0	9.0	
87BRpH01	0.832			1		0.931		0.1/0.1
87BRpH02	0.836			1			0.875	0.1/0.1
87BRpH03	0.862	1.041		1			0.846	0.1/0.1
87BRpH04				1		0.956	0.908	0.1/0.1
87BRpH05	0.846	0.966		1				0.1/0.1
87BRpH06	0.855			1		0.926	0.746	0.1/0.1
87BRpH07	0.903	0.998		1				0.1/0.1
87BRpH08				1		0.942	0.897	0.1/0.1
87BRpH09	0.783			1		0.906	0.734	0.1/0.1
87BRpH10			0.939	1		0.951		0.1/0.1
87BRpH11				1	1.005			0.1/0.1
87BRpH11				1	0.915			0.03/0.1
87BRpH11				1	0.978			0.3/0.1
87BRpH11				1	0.917			1.0/0.1
87BRpH12				1	0.998			0.1/0.1
87BRpH12				1	1.061			0.03/0.1
87BRpH12				1	1.006			0.3/0.1
87BRpH12				1	0.994			1.0/0.1
87BRpH13			0.987	1				0.1/0.1
87BRpH13			0.916	1				0.03/0.1
87BRpH13			0.998	1				1.0/0.1
Average	0.845	1.002	0.960	1	0.984	0.935	0.834	
SD	0.035	0.031	0.034		0.045	0.017	0.070	

[a] BP^{p7}: Breakdown potential at $pH_o = 7$.

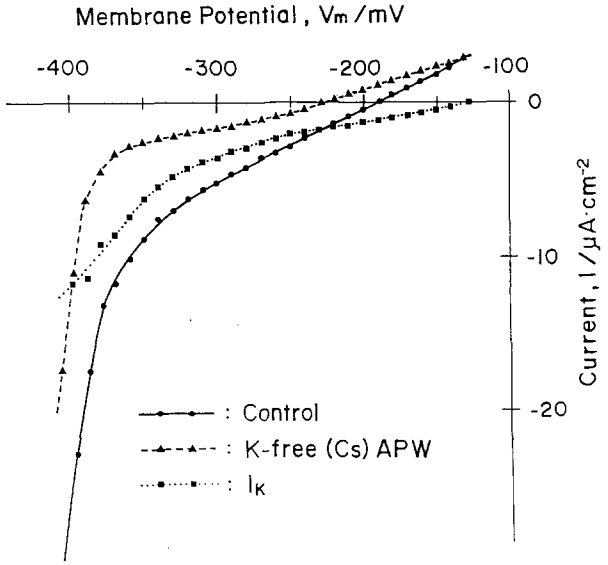

Fig. 9. Effect of K^+ on the breakdown phenomenon. K^+ in the standard APW (*s*-APW) was exchanged for Cs^+. Three I-V_m relationships, i.e., the control (in *s*-APW), the one in K-free (Cs) APW, and I_K-V_m relationship, are shown. The last relationship is obtained by subtracting the I-V_m relationship in K-free (Cs) APW from the control one

(Cs) APW and the control one. The I_K-V_m relationship crosses at -128 mV with the V_m-axis. This V_m value is in the range of K^+ equilibrium potential ($E_K = -100 \sim -140$ mV)) of the *Characeae* plasmalemma. The I_K-V_m relationship shows a slight rectification in the V_m range between -128 and -250 mV. In the more negative V_m region it shows a slight inward-going rectification. In the same V_m region the inward-going current of the I-V_m relationship in the K-free (Cs) APW is so marked that both I-V_m relationships cross at -410 mV.

Discussion[8]

In this communication we have described a large positive E_m shift during the large inward current

[8] In this paper the intracellular ionic composition of *Chara* internode, necessary for the estimation of equilibrium potentials, were taken from the following sources: MacRobbie (1962), Spanswick and Williams (1964), Kishimoto and Tazawa (1965), Coster and Hope (1968), Kitasato (1973), and Tazawa, Kishimoto and Kikuyama (1974).

flow in the breakdown region. Although such a large positive E_m value beyond +50 mV (Figs. 2 or 4) was not always observed, a positive E_m shift in the breakdown region was always observed when the membrane was released from voltage clamp conditions during a negative shift of V_m.

The cause of a large E_m shift to a positive level is the increase of either G_{Cl} or G_{Ca} or both, because the ion species the equilibrium potential of which is beyond +50 mV is restricted to Cl^- (E_{Cl} = +55 ~ +95 mV) and Ca^{2+} (E_{Ca} = +65 ~ +85 mV). Upon excitation on the positive side in the *Characeae* internode, a sudden cessation of cytoplasmic streaming is usually observed. Although this cessation is intimately related to an increase in the cytoplasmic Ca^{2+} (Williamson & Ashley, 1982), the measured Ca^{2+} inflow as ion carrier during excitation is as small as 0.1 to 0.4 $\mu A/cm^2$ (Hayama, Shimmen & Tazawa, 1979, Kikuyama & Tazawa, 1983). On the other hand, in the V_m range more negative than BP the cytoplasmic streaming generally loses its rate of speed and finally stops, but sudden cessation of the cytoplasmic streaming never occurs (visibly) during the large inward current flow (10 to 30 $\mu A/cm^2$). This observation suggests that the amount of Ca^{2+} inflow during the breakdown phenomenon should be usually less than that observed during action potential.

In contrast with the small Ca^{2+} influx, the reported Cl^- efflux during action potential (about 150 to 10000 $pmol/cm^2$/impulse; Gaffey & Mullins, 1958; Mailman & Mullins, 1966; Oda, 1976) almost coincides with the peak of a transient inward current under voltage clamp (10 to 100 $\mu A/cm^2$; Kishimoto, 1964; Tsutsui, 1989). Similar to the case of excitation upon depolarization, a large Cl^- efflux (about 1000 $pmol/cm^2$/sec) occurs in the breakdown region which corresponds to about 100 $\mu A/cm^2$ of the inward current (Coster & Hope, 1968). Thus, the main ion carrier which causes a large positive E_m shift is Cl^-, not Ca^{2+}.

Judging from a pioneering work by Shimmen and Tazawa (1980) on the tonoplast-free cell internally perfused with EGTA (Shimmen, Kikuyama & Tazawa, 1976; Shimmen & Tazawa, 1977), the selectivity of tonoplast-free cell membrane to various anions seems to be very complicated, though they simply assumed that the tonoplast-free cell membrane behaves as a Cl^- electrode at the depolarized state. According to our unpublished data, in the tonoplast-free cell internally perfused with Cl^--free and SO_4^{2-} solution, the level of E_m shift during the breakdown phenomenon appeared at about −100 mV. This could be, to some extent, understood by assuming that the membrane was less permeable to SO_4^{2-} than to Cl^-, since E_{Cl} was largely negative, while E_{SO_4} largely positive under the above condition. Nevertheless, to our regret, we have been still unable to find a stable internal environment for the study of the electrical tolerance in the tonoplast-free cell.

It should be kept in mind that monovalent cations such as K^+ and Na^+ have almost no effect on the BP level (Figs. 8 and 9), while divalent cations such as Ca^{2+} and Mg^{2+} have great effect (Ohkawa & Tsutsui, 1988*a,b*; *see also* Table 1 in the present paper). However, as ion carrier, K^+ contributes partly to the large inward current (Fig. 9), while Na^+ current is very small (Fig. 8). The I-V_m relationship which is obtained by subtracting the I-V_m curve in K-free (Cs) APW from the control I-V_m relationship crosses with the V_m-axis at −128 mV (Fig. 9). This V_m level is in the most reliable range of E_K in the *Characeae* plasmalemma. This indicates that Cs^+ blocks K^+ channel specifically (Sokolik & Yurin, 1986; Tester, 1988*a,b*). Accordingly, we can consider the differential I-V_m relationship as the I_K-V_m relationship. In Fig. 9, the K^+ inflow increases gradually in the V_m region more negative than −340 mV (which is still less negative than BP), i.e., G_K increases. This increase in G_K can cause a positive E_m shift up to E_K (−100 ~ −140 mV), but cannot be the cause of a large positive E_m shift beyond 0 mV.

Since Cs^+ blocks the K^+ channel specifically, it is most reasonable to suppose that the negative shift of the resting potential caused by the exchange of K^+ for Cs^+ (Fig. 9) is mainly due to the relative increase of the ratio of pump conductance (G_p) to G_K. The reason is that the electromotive force of the electrogenic H^+ pump, E_p, is more negative than the resting potential (about −200 to −300 mV: Kishimoto et al., 1984; more negative than −400 mV: Beily, 1984). On the other hand, since G_p itself decreases voltage dependently in the V_m range more negative than the resting potential (Kishimoto et al., 1984; Takeuchi et al., 1985), the rectification pattern (i.e., decrease of the rate of increase of the inward current) between −230 and −350 mV shown in the I-V_m relationship in K-free (Cs) APW is caused by the voltage-dependent decrease in G_p. Actually, the I-V_m relationship in K-free (Cs) APW resembles a part of the I_p-V_m relationship of H^+ pump current in the V_m range between −150 and −350 mV (Kishimoto et al., 1984).

It is interesting in the *Chara* plasmalemma that the inductive property is pronounced during the breakdown phenomenon (Fig. 2*B*), while the capacitative property is marked during excitation on the positive side (Kishimoto et al., 1982). In Eqs. (4) and (9), if a change in the membrane capacitance occurs during the breakdown phenomenon, it causes a change in the time constant which affects the time process of initial capacity current, but thereby the tail current of i_{off} never changes its sign

against that of the off-spike. Besides, the change in time course of the capacity current is actually slight in Fig. 3, though more detailed experiments and analyses are needed to be done in the future.

Coster and Smith (1977) reported that in the *Chara* plasmalemma the membrane impedance becomes occasionally inductive at very low frequency (less than 1 Hz) in the breakdown region. According to them, an electro-osmotic water flow might cause depletion of ions in the neighborhood of the surface of membrane, which builds up a diffusion potential different from that expected between the cytoplasm and the bulk solution. This newly established diffusion component might induce an inductive property by causing a phase lag of the current response against an applied voltage (Coster & Smith, 1977). We tried to determine to what extent an electro-osmosis is related to the breakdown phenomenon by varying external osmotic concentration. Varying the external osmotic concentration by mixing *s*-APW with 200 mM sorbitol-APW had no effect on neither resting potential nor on the I-V_m relationship (four samples; *data not shown*). Thus, our conclusion is that the effect of electro-osmosis on the breakdown phenomenon may be very little, if any.

Our data regarding the effect of pH_o on the BP level (Fig. 7) resemble those obtained by Ross, Ferrier and Dainty (1985, Fig. 5 of their paper) who demonstrated the inductive property by showing the relation between pH_o and frequency at which the phase shift between voltage and current perturbation becomes zero. They introduced theoretically a possible mechanism of inductive property of the membrane by assuming that in the bulk medium ions (mainly H^+ or OH^-) will be carried by diffusion, while in the extracellular stagnant layer they will be driven by electrical potential difference. Though the current driven by electrical potential difference follows it without a time lag, the current carried by diffusion will lag the former current (Ferrier, et al., 1985). Although such a theoretical consideration is attractive, we suppose, on the basis of the data on both Ca^{2+} and Ca^{2+}/Mg^{2+} ratio dependence of the BP level (Ohkawa & Tsutsui, 1988*a*,*b*), that the binding constant of Ca^{2+} with the Ca^{2+} binding site should be affected by pH_o. It is expected that Ca^{2+} binds with the Ca^{2+} binding site most strongly around $pH_o = 7$ and the membrane is electrically most tolerant, although our expectation of pH_o on the BP/BP^{p7} ratio was that the ratio would be larger than 1 when pH_o was higher than 7.0.

The experiments shown in Figs. 3 and 5 give us some information on the inductive property of the membrane, though the amplitude of v_o in this case is considerably large. As shown in Fig. 10*A*, the current on-response having inductive property was generally well fitted by the following equation (*see also* Appendix):

$$i_{on} = i_c + G \cdot v_o + \overline{g(v)} \cdot [1 - \exp(-t/\tau_1)]^n \cdot v_o \quad (14)$$

where, i_c is the initial capacitive current, G the instantaneous chord (DC) conductance at V_m, and $\overline{g(v)}$, not the change in G itself, is the apparent steady-state value of the change in G. τ_1 is the time constant of the inductive current, which essentially originates from the changing process from G to $G + g^v$ (where, $\overline{g^v} = \sum \overline{g_i^v}$; *see* Eq. (A10)). Note that the time course of e, i.e., the change in E_m, is generally more complicated than that of i_{on} (Eqs. (A5), (A8) and (A10)).

When V_m of the *Chara* plasmalemma was held at around BP level, the ranges of τ_1 and n in Eq. (14) were between about 30 and 70 msec and between 2 and 3, respectively (Fig. 10*A*), though n was not always an integer (the average n for eight experimental results of three samples was 2.4). The time constant of the inductive off-response was almost the same as that of the on-response (Fig. 10*B*). Although at present we cannot explain why n is not always an integer[9], if n is an integer (i.e., 2 or 3), the time domain analysis by using Eq. (14) can be easily transformed to the frequency domain by using Fourier transformation. In that case we must be very careful in interpreting the data of impedance measurement obtained by applying an AC current or voltage perturbation; because of voltage dependence of G the behavior of G will differ according to the sign of v_o, even if its amplitude is the same.

By the analogy with the voltage-dependent K^+ channel in the squid giant axon membrane which is well known as one of the typical inductive properties of the membrane (Hodgkin & Huxley, 1952; Cole, 1968), the inductive property observed during the breakdown phenomenon in the *Chara* plasmalemma should be intimately related to opening or breakdown kinetics of the Cl^- channel. Because, the fact that the inductive current was simulated by Eq. (A12) may strongly suggest that the measured change in G in the breakdown region is not due to changes of various conductances, but due only to change of one specific ion channel conductance, most likely G_{Cl}. If so, in Eqs. (14) and (A12) we can suppose $\overline{g(v)}$ as $\overline{g_{Cl}(v)}$ (*see* Appendix and Fig. 10). The $\overline{g(v)}$ values used for the simulation in Fig. 10 were 4.91, 25.39 and 22.86 $\mu S/cm^2$ to -32.0, -37.1

[9] One of the reasons might be due to the neglect of K^+ currents which are slightly inductive (*cf.* Fig. 9).

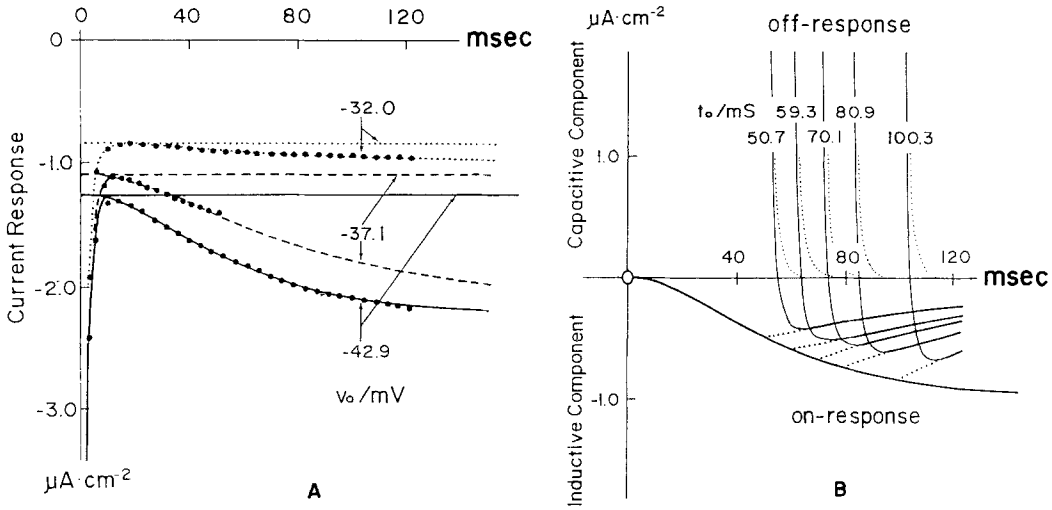

Fig. 10. Simulated inductive current responses. (*A*) Simulation for on-responses (i_{on}) to three different v_o in Figs. 3 and 5. The equation used for the simulation is: $i_{on} = i_c + G \cdot v_o + \overline{g(v)} \cdot [1 - \exp(-t/\tau_1)]^{2.5} \cdot v_o$, where i_c is the initial capacity current, $G \cdot v_o$ the DC current, and $\overline{g(v)} \cdot [1 - \exp(-t/\tau_1)]^{2.5} \cdot v_o$ the inductive current. Since the DC current component is constant, it is shown as a straight line parallel to the time axis. Since i_c is superimposed on the DC current, i_c decays to the level of the DC current, not to zero. G and $\overline{g(v)}$ are: 26.27 and 4.91 μS/cm^2 for $v_o = -32.0$ mV, 29.62 and 25.39 μS/cm^2 for $v_o = -37.1$ mV, and 29.45 and 22.86 μS/cm^2 for $v_o = -42.9$ mV, respectively. τ_1 is: 47.6 msec for $v_o = -32.0$ and -37.1 mV and 36.2 msec for $v_o = -42.9$ mV. (●): data points; (·····): simulation for i_{on} to $v_o = -32.0$ mV; (----): simulation for i_{on} to $v_o = -37.1$ mV; and (—): simulation for i_{on} to $v_o = -42.9$ mV. (*B*) The continuity of inductive components of off-responses to the ends of on-responses. To avoid complexity, i_c and DC components of the on-response are not shown and only the inductive component of the on-response simulated to $v_o = -42.9$ mV in *A* is shown (solid line). A set of five solid lines of off responses in data shown in Fig. 5. Dotted points (·····) show decay of the inductive components, which were drawn by eye. Capacitive current (·····) was drawn by subtracting each inductive component from each off-response

-42.9 mV of v_o, respectively. By assuming that E_{Cl} is $+70$ mV, at $V_m = -375$ mV the change in G_{Cl} (g^v_{Cl}) is estimated to be 0.3294, 1.9539 and 2.0100 μS/cm^2 to -32.0, -37.1 -42.9 mV of v_o, respectively, since $\overline{g_{Cl}(v)} = \overline{g^v_{Cl}} \cdot [1 + (V_m - E_{Cl})/v_o]$ (Eq. (A11)). Thus, the change in G_{Cl}, i.e., g^v_{Cl}, is actually small. However, this slight change in G_{Cl} can be apparently amplified by the factor of $[1 + (V_m - E_{Cl})/v_o]$ during impedance measurement. Thus, $g_{Cl}(v)$ is apparent change in G_{Cl}. Such a change in G_{Cl} should be attributed to the rearrangement of the membrane molecular structure in response to an applied high voltage as discussed by Mullins (1959). Since K^+ currents also appear to be slightly inductive (Fig. 9), more detailed experiments are needed to explain the above aspect of the ionic process in the *Chara* plasmalemma.

The following difference in the current amount in Fig. 3 is noteworthy: At $V_m = -375$ mV, I is about -10 μA/cm^2 and i_s (steady-state value of i_{on}) at v_o of -42.9 mV is about -2.3 μA/cm^2. Nevertheless, I at $V_m = -412.9$ ($= -375-42.9$) mV is about -20 μA/cm^2, not -12.3 ($= -10-2.3$) μA/cm^2. Since the I-V_m relationship under a slow ramp potential control almost corresponds to the steady-state I-V_m relationship (Ohkawa & Tsutsui, 1988*a*), we suppose that another much slower process is involved in the increase of G, the time constant of which will be perhaps a few seconds. This process is comparable to the frequency range where the inductive property is usually observed (Coster & Smith, 1977; Beilby & Beilby, 1983; Ross et al., 1985).

We would like to thank emeritus Prof. U. Kishimoto and Dr. N. Kami-ike for their critical readings and discussions and also thanks to Dr. S.A. Salehi for his correction of our manuscript. This work has been supported by a Research Grant (63480511) from the Ministry of Education, Science and Culture of Japan.

References

Beilby, M.J. 1984. Current-voltage characteristics of the proton pump at *Chara* plasmalemma: I. pH dependence. *J. Membrane Biol.* **81**:113–125

Beilby, M.J. 1986. Potassium channels and different states of *Chara* plasmalemma. *J. Membrane Biol.* **89**:241–249

Beilby, M.J., Beilby, B.N. 1983. Potential dependence of the admittance of *Chara* plasmalemma. *J. Membrane Biol.* **74**:229–245

Cole, K.S. 1968. Membranes, Ions and Impulses. University of California Press, Berkeley

Coster, H.G.L. 1965. A quantitative analysis of the voltage-current relationships of fixed charge membranes and the associated property of "punch-through". *Biophys. J.* **5**:669–686

Coster, H.G.L., Hope, A.B. 1968. Ionic relations of cells of *Chara australis*. XI. Chloride fluxes. *Aust. J. Biol. Sci.* **21**:243–254

Coster, H.G.L., Smith, J.R. 1977. Low-frequency impedance of *Chara corallina:* Simultaneous measurement of the separate plasmalemma and tonoplast capacitance and conductance. *Aust. J. Plant Physiol.* **4**:667–674

Ferrier, J.M., Dainty, J., Ross, S.M. 1985. Theory of negative capacitance in membrane impedance measurements. *J. Membrane Biol.* **85**:245–249

Fisahn, J., Hansen, U.-P., Gradmann, D. 1986*a*. Determination of charge, stoichiometry and reaction constants from *I-V* curve studies on a K^+ transporter in *Nitella*. *J. Membrane Biol.* **94**:245–252

Fisahn, J., Mikschl, E., Hansen, U.-P. 1986*b*. Separate oscillations of the electrogenic pump and of a K^+-channel in *Nitella* as revealed by simultaneous measurement of membrane potential and of resistance. *J. Exp. Bot.* **37**:34–47

Gaffey, C., Mullins, L.J. 1958. Ion fluxes during the action potential in *Chara*. *J. Physiol. (London)* **144**:505–524

Hayama, T., Shimmen, T., Tazawa, M. 1979. Participation of Ca^{2+} of cytoplasmic streaming induced by membrane excitation in *Characea* internodal cells. *Protoplasma* **99**:305–321

Hodgkin, A.L., Huxley, A.F. 1952. A quantitative description of membrane current and its application to conduction and excitation in nerve. *J. Physiol. (London)* **117**:500–544

Kami-ike, N., Ohkawa, T., Kishimoto, U., Takeuchi, Y. 1986. A kinetic analysis of the electrogenic pump of *Chara corallina:* IV. Temperature dependence of the pump activity. *J. Membrane Biol.* **94**:163–171

Kikuyama, M., Tazawa, M. 1983. Transient increase of intracellular Ca^{2+} during excitation of tonoplast-free *Chara* cells. *Protoplasma* **117**:62–67

Kishimoto, U. 1964. Current voltage relations in *Nitella*. *Jpn. J. Physiol.* **14**:515–527

Kishimoto, U., Kami-ike, N., Takeuchi, Y., Ohkawa, T. 1982. An improved method for determining the ionic conductance and capacitance of the membrane of *Chara corallina*. *Plant Cell Physiol.* **23**:1041–1054

Kishimoto, U., Kami-ike, N., Takeuchi, Y., Ohkawa, T. 1984. A kinetic analysis of the electrogenic pump of *Chara corallina:* I. Inhibition of the pump by DCCD. *J. Membrane Biol.* **80**:175–183

Kishimoto, U., Tazawa, M. 1965. Ionic composition of the cytoplasm of *Nitella flexilis*. *Plant Cell Physiol.* **6**:507–518

Kitasato, H. 1973. K permeability of *Nitella clavata* in the depolarized state. *J. Gen. Physiol.* **62**:535–549

MacRobbie, E.A.C. 1962. Ionic relation of *Nitella translucens*. *J. Gen. Physiol.* **45**:861–878

Mailman, D.S., Mullins, L.J. 1966. The electrical measurement of chloride fluxes in *Nitella*. *Aust. J. Biol. Sci.* **19**:385–398

Mullins, L.J. 1959. An analyis of conductance changes in squid axon. *J. Gen. Physiol.* **42**:1013–1035

Oda, K. 1976. Simultaneous recording of potassium and chloride effluxes during an action potential in *Chara corallina*. *Plant Cell Physiol.* **17**:1085–1088

Ohkawa, T., Kishimoto, U. 1977. Breakdown phenomena in the *Chara* membrane. *Plant Cell Physiol.* **18**:67–80

Ohkawa, T., Tsutsui, I. 1988*a*. Electrical tolerance (breakdown) of the *Chara corallina* plasmalemma: I. Necessity of Ca^{2+}. *J. Membrane Biol.* **103**:273–282

Ohkawa, T., Tsutsui, I. 1988*b*. Electrical tolerance of the *Chara* plasmalemma. *In:* The Ion Pumps: Structure, Function, and Regulation. W.D. Stein, editor. p. 6. Alan R. Liss, New York

Ohkawa, T., Tsutsui, I., Kishimoto, U. 1986. K^+ channel in the *Chara* plasmalemma: Estimations of K^+ channel density and single K^+ channel conductance. *Plant Cell Physiol.* **27**:1429–1438

Ross, S.M., Ferrier, J.M., Dainty, J. 1985. Frequency-dependent membrane impedance in *Chara corallina* estimated by Fourier analysis. *J. Membrane Biol.* **85**:233–243

Shimmen, T., Kikuyama, M., Tazawa, M. 1976. Demonstration of two stable potential states of plasmalemma of *Chara* without tonoplast. *J. Membrane Biol.* **30**:249–270

Shimmen, T., Tazawa, M. 1977. Control of membrane potential and excitability of *Chara* cells with ATP and Mg^{2+}. *J. Membrane Biol.* **37**:167–192

Shimmen, T., Tazawa, M. 1980. Intracellular chloride and potassium ions in relation to excitability of *Chara* membrane. *J. Membrane Biol.* **55**:223–232

Sokolik, A.I., Yurin, V.M. 1986. Potassium channels in plasmalemma of *Nitella* cells at rest. *J. Membrane Biol.* **89**:9–22

Spanswick, R.M., Williams, E.J. 1964. Electrical potential and Na, K, and Cl concentration in the vacuole and cytoplasm of *Nitella translucens*. *J. Exp. Biol.* **15**:193–200

Takeuchi, Y., Kishimoto, U., Ohkawa, T., Kami-ike, N. 1985. A kinetic analysis of the electrogenic pump of *Chara corallina:* II. Dependence of the pump on the external pH. *J. Membrane Biol.* **86**:71–26

Tazawa, M., Kishimoto, U., Kikuyama, M. 1974. Potassium, sodium and chloride in the protoplasm of *characeae*. *Plant Cell Physiol.* **15**:103–110

Tester, M. 1988*a*. Blockade of potassium channels in the plasmalemma of *Chara corallina* by tetraethylammonium, Ba^{2+}, Na^+, and Cs^+. *J. Membrane Biol.* **105**:77–85

Tester, M. 1988*b*. Potassium channels in the plasmalemma of *Chara corallina* are multi-ion pores: Voltage-dependent blockade by Cs^+ and anomalous permeabilities. *J. Membrane Biol.* **105**:87–94

Tsutsui, I. 1989. Role of Ca^{2+} in excitable channels and electrogenic pumps in *Chara* plasmamembrane and other cells. In: Role of Calcium in Biological Systems. L.J. Anghileri, editor. Vol. 5. CRC Press, Boca Raton (FL) (*in press*)

Williamson, R.E., Ashley, C.C. 1982. Free Ca^{2+} and cytoplasmic streaming in the alga *Chara*. *Nature (London)* **296**:647–651

Received 12 July 1989; revised 29 September 1989

Appendix

Inductance Due to Voltage-Dependent Change in *G*

When R_s value is much smaller than R_m ($= 1/G_m$) value, we can approximate G as G_m. Then, in Eqs. (10) and (11) G and E_m are as follows:

$$G = \Sigma G_i \tag{A1}$$

$$E_m = \Sigma G_i \cdot E_i / \Sigma G_i \tag{A2}$$

where G_i and E_i are the conductance and the equilibrium potential of i species ion, respectively.

For simplicity, let us consider that a small stepwise potential change v is superimposed at the steady state of the membrane at V_m. Thereby, each channel will change from the existing steady state to a new steady state. Respective channels have

different voltage and time dependence. Thus, let g_i be a small change in G_i caused by v. Similarly, let i and e be deviations of the current I and E_m caused by v, respectively.

$$I + i = \Sigma(G_i + g_i) \cdot [(V_m + v) - (E_m + e)] \tag{A3}$$

where,

$$E_m + e = \Sigma(G_i + g_i) \cdot E_i / \Sigma(G_i + g_i). \tag{A4}$$

Accordingly,

$$e = \Sigma g_i \cdot (E_i - E_m) / \Sigma(G_i + g_i) \tag{A5}$$

$$i = \Sigma G_i \cdot v + \Sigma g_i \cdot (V_m + v - E_m) - \Sigma(G_i + g_i) \cdot e. \tag{A6}$$

From Eqs. (A1), (A5) and (A6),

$$i = [G + g(v, t)] \cdot v \tag{A7}$$

where,

$$g(v, t) = \Sigma g_i \cdot [1 + (V_m - E_i)/v] = \Sigma g_i(v, t) \tag{A8}$$

$$g_i(v, t) = g_i \cdot [1 + (V_m - E_i)/v]. \tag{A9}$$

It should be noticed that $g_i(v, t)$ in Eq. (A9) and $g(v, t)$ in Eq. (A8) differ from g_i and Σg_i, respectively. In Eqs. (A8) and (A9), V_m and v can be kept constant under voltage clamp conditions and E_i is equilibrium potential of i species of ion. If no change in G_i is caused by v, Eq. (A7) expresses a simple ohmic relationship, i.e., $i = G \cdot v$, when $i_{on} = i_c + G \cdot v$ (*cf.* Eq. (4)). However, the change in G during an impedance measurement in the breakdown region is actually marked. If we can split g_i (i.e., term of the change in G_i) into functions of voltage, $\overline{g_i^v}$, and time, $y_i(t)$, then $g_i = \overline{g_i^v} \cdot y_i(t)$. By comparing this relation to Eq. (A9), we can get the following relation:

$$g_i(v, t) = \overline{g_i^v} \cdot [1 + (V_m - E_i)/v] \cdot y_i(t) = \overline{g_i(v)} \cdot y_i(t) \tag{A10}$$

where

$$\overline{g_i(v)} = \overline{g_i^v} \cdot [1 + (V_m - E_i)/v]. \tag{A11}$$

Taking these relations into account, we tried a simulation for such inductive component (i_1) as shown in Figs. 3 and 5 using a much simplified form, that is,

$$i_1 = g(v, t) \cdot v$$

$$= \overline{g(v)} \cdot [1 - \exp(-t/\tau_1)]^n \cdot v. \tag{A12}$$

Thus, the current on-response is: $i_{on} = i_c + g \cdot v + i_1$. The result of simulations is shown in Fig. 10.